ISSN 0036-0295, Russian Metallurgy (Metally), Vol. 2024, No. 2, pp. 298–304. © Pleiades Publishing, Ltd., 2024.
Russian Text © The Author(s), 2023, published in Deformatsiya i Razrushenie Materialov, 2023, No. 11, pp. 33–39.

## STRUCTURE AND PROPERTIES OF THE DEFORMED STATE

*In loving memory of Aleksandr Markovich Glezer*

# Formation of Gradient Structural-Phase States in the Head of Special-Purpose Rails during Operation

**Yu. F. Ivanov[a], M. A. Porfir'ev[b], V. E. Gromov[b, *], R. E. Kryukov[b], and Yu. A. Shlyarova[b]**

[a] *Institute of High-Current Electronics, Siberian Branch, Russian Academy of Sciences, Tomsk, 634055 Russia*

[b] *Siberian State Industrial University, Novokuznetsk, 654007 Russia*

**e-mail: gromov@physics.sibsiu.ru*

Received April 28, 2023; revised May 18, 2023; accepted May 23, 2023

**Abstract**—The structure, phase composition, and dislocation substructure in the head of long differentially quenched special-purpose rails made of E90KhAF steel after a passed gross tonnage of 187 mln t are analyzed. The formation of flexural extinction contours is observed, which indicates an elastic-stressed state in the material. The sources of lattice curvature–torsion are found to be intra- and interphase boundaries, and the mechanisms of destruction of cementite lamellae are determined.

**Keywords:** rails, E90KhAF steel, scalar dislocation density, pearlite, cementite

**DOI:** 10.1134/S0036029524700575

## INTRODUCTION

According to the data of OAO Russian Railways, the main causes of the removal of rails are contact-fatigue defects and surface wear. Numerous investigations have shown that a critical dislocation density, the formation of white surface layers, the transformation of a carbide phase, and a high surface microhardness are observed in the near-surface layers of rails in this case [1–11].

Three years ago, AO Evraz ZSMK started the production of special-purpose DT400IK rails with increased wear resistance and back-to-back endurance. To improve differentiated quenching conditions for such rails in order to form high operational properties, it is necessary to understand the nature and laws of formation of the structural-phase states in the surface layers of rails after various volumes of tonnage passed.

The purpose of this work is to analyze the formation of gradients of structural-phase states and dislocation substructures in the surface layers of the rail head made of E90KhAF hypereutectoid steel after operation.

## EXPERIMENTAL

We studied samples of differentially quenched DT400IK rails made of E90KhAF steel produced by AO Evraz ZSMK after operation on the experimental ring of AO VNIIZhT (gross tonnage of 187 mln t). The elemental composition of steel is regulated by GOST 51685–2013 and TU 24.10.75111-298-057576.2017 of Russian Railways.

According to them, the mass fractions of the elements are (%) 0.83–0.95 C, 0.75–1.25 Mn, 0.25–0.60 Si, 0.08–0.15 V, 0.20–0.60 Cr, 0.010–0.020 N, <0.020 P, <0.020 S, and <0.004 Al.

The morphology of a structure and phase composition and a dislocation substructure (scalar dislocation density, lattice curvature [12]) were determined by transmission electron microscopy (JEOL JEM-2100F microscope), as in [9–11], in the fillet of the rail head at distances of 0, 2, and 10 mm from the surface.

## RESULTS AND DISCUSSION

The structure of steel in its initial state is represented by grains of pearlite of predominantly lamellar morphology and a small amount of primary cementite. The pearlite grain size is 0.6–3 μm (Fig. 1).

After long-term operation, a dislocation substructure is observed in the ferrite lamellae of pearlite colonies: these are mainly chaotically distributed dislocations (Fig. 2a) and dislocation networks (Fig. 2b).

The scalar dislocation density $\langle\rho\rangle$ increases as the fillet surface of the rail head is approached and reaches a maximum value at a distance of 2 mm from the surface (Fig. 3a).

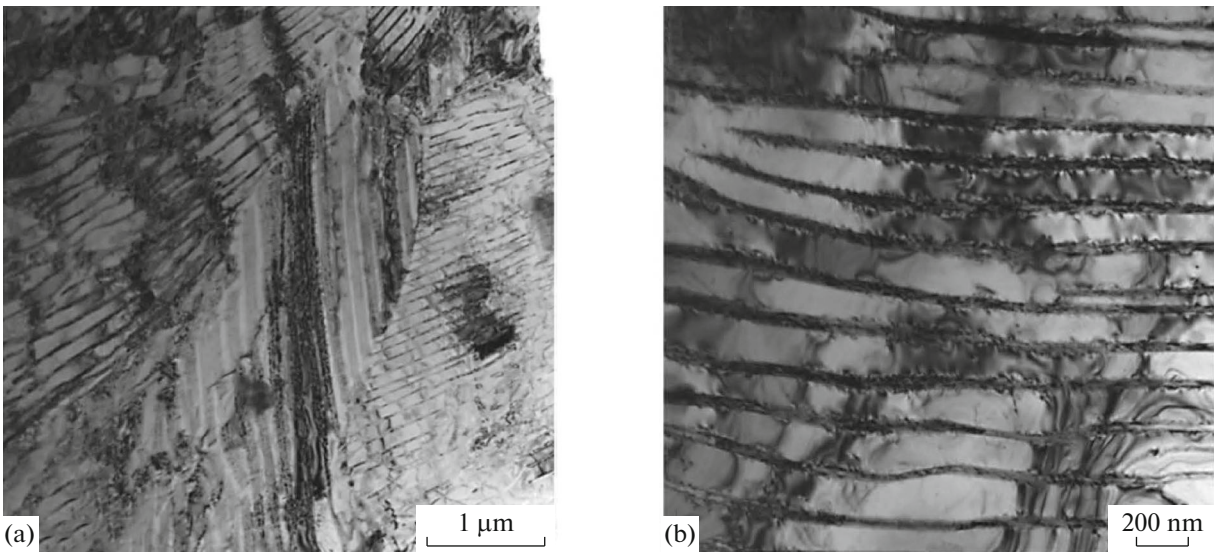


**Fig. 1.** Structure of rail steel in its initial state ((a) scanning and (b) transmission electron microscopy).

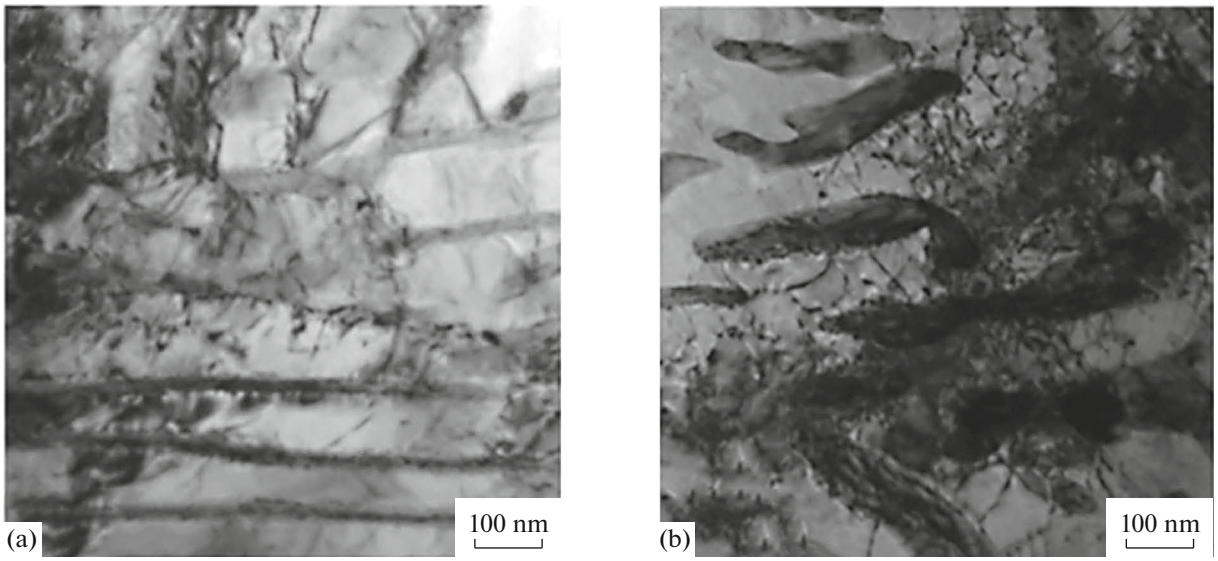


**Fig. 2.** Dislocation substructure of the ferrite lamellae of pearlite colonies.

Ferritic lamellae are fragmented. The transverse fragment size is limited to the distance between cementite lamellae and weakly changes with the distance from the surface, unlike longitudinal size $D$, which increases with the distance from the surface (Fig. 3b). The structure of the cementite lamellae is also fragmented, and longitudinal fragment size $d$ increases with the distance from the surface (Fig. 3c).

Bending extinction contours are present on electron-microscopic images of the structure, which indicates lattice curvature–torsion. The sources of curvature–torsion are grain boundaries or pearlite colony boundaries, as well as ferrite and cementite lamella boundaries. In the first case, a bend contour (contour of the first type) crosses a grain or a pearlite colony from one grain boundary (colony) to another (Fig. 4a). In the second case, a bend contour (contour of the second type) is located within a single ferrite or cementite lamella (Fig. 4b).

The lattice curvature–torsion in the rail metal was estimated using the average contour thickness (transverse sizes) and the specific contour density (the number of contours per unit foil area). Note that the average transverse sizes of the extinction contours of both types change nonmonotonically with the distance

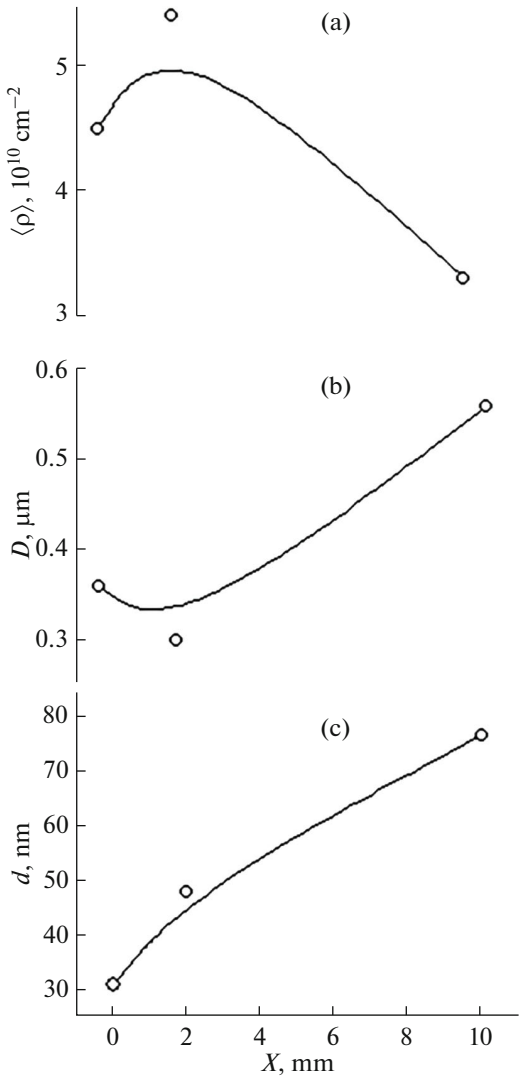


**Fig. 3.** (a) Scalar dislocation density, (b) longitudinal size of ferrite lamella fragments, and (c) longitudinal size of cementite lamella fragments vs. the distance from the fillet surface.

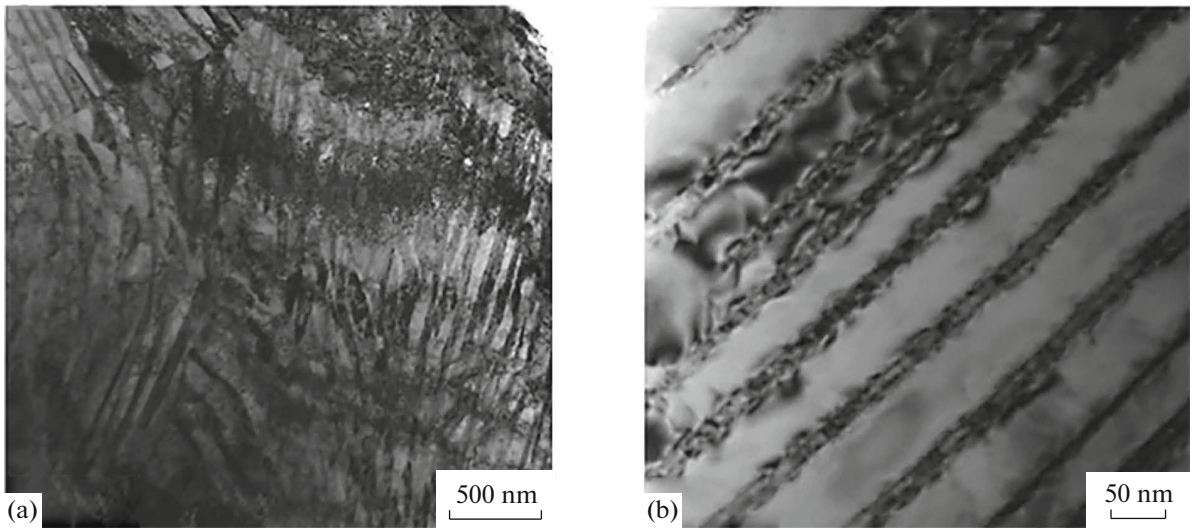


**Fig. 4.** Electron-microscopic images of bend extinction contours of the (a) first and (b) second type in ferrite lamellae.

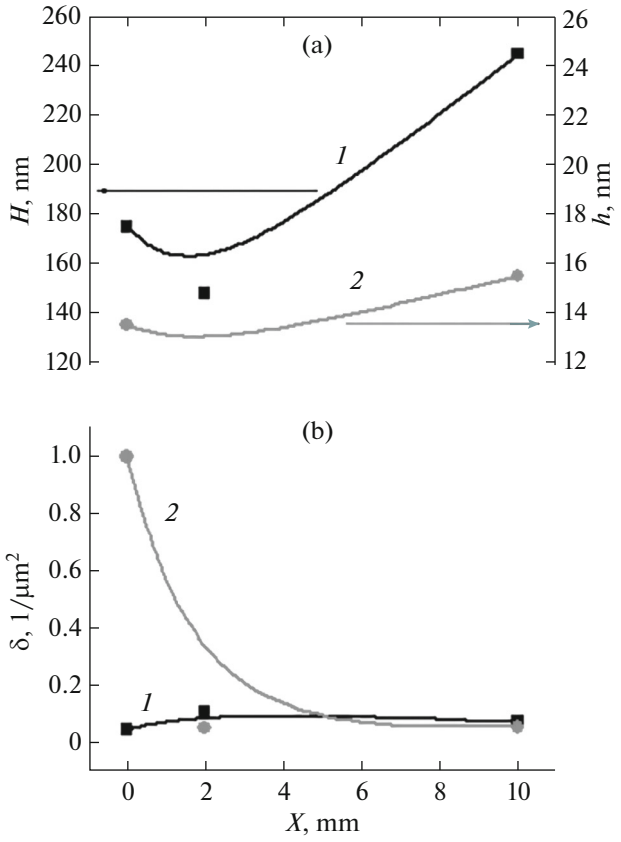


**Fig. 5.** (a) Transverse sizes of bend extinction contours and (b) their specific density vs. the distance from the fillet surface: (*1*, *2*) first and second types of bend extinction contours, respectively.

from the fillet surface and reach minimum values at a depth of 2 mm (Fig. 5a).

Taking into account well-known facts indicating an inversely proportional dependence of the transverse contour sizes on the internal stresses in a material [1, 10, 11], we can state that the subsurface layer of rails is most strongly stressed. The stress amplitude having formed at interphase boundaries (interface between cementite and ferrite lamellae) is an order of magnitude higher than the stress amplitude having formed at the intraphase boundaries (pearlite grain boundaries). The pronounced distance dependence of the density of second-type contours (Fig. 5b), which reaches a maximum at the fillet surface ($X = 0$), indicates a high density of stress concentrators at interphase boundaries.

Extinction contours are less frequently observed in cementite lamellae. The transverse sizes of such contours are almost independent of the distance from the fillet surface and are 8–13 nm.

The deformation action on the structure of lamellar pearlite at high degrees of deformation is accompanied by the destruction of cementite lamellae. It occurs according to the following two main mechanisms: (i) dissolution accompanied by the motion of carbon atoms to dislocation cores and, then, to the volume of ferritic lamellae and the subsequent formation of globular carbide phase nanoparticles there; (ii) cutting of cementite lamellae by moving dislocations and the subsequent motion of fragments in the volume of a deformed pearlite grain [12–14]. In the limiting case, the refinement of cementite lamellae leads to their dissolution. According to classical concepts, carbon diffusion occurs in the stress field created by a dislocation substructure, which forms around cementite lamellae. Here, the degree of cementite decomposition is usually determined by the dislocation density and the type of substructure [13].

When carbon atoms are "pulled" out of the crystal lattice, the defect substructure of carbide changes due to the penetration of dislocations into the cementite lattice. However, the incoherent α-Fe–$Fe_3C$ interface would prevent this, leaving only diffusive mass transfer possible [1, 14]. It can occur according to various mechanisms: diffusion through interstices and along deformation vacancies [15, 16].

Both mechanisms of cementite destruction were revealed in the surface layer of the fillet: dissolution and destruction by cutting by moving dislocations (Fig. 6). In the layer located at a distance of 2 mm from the surface, the main mechanism of destruction of

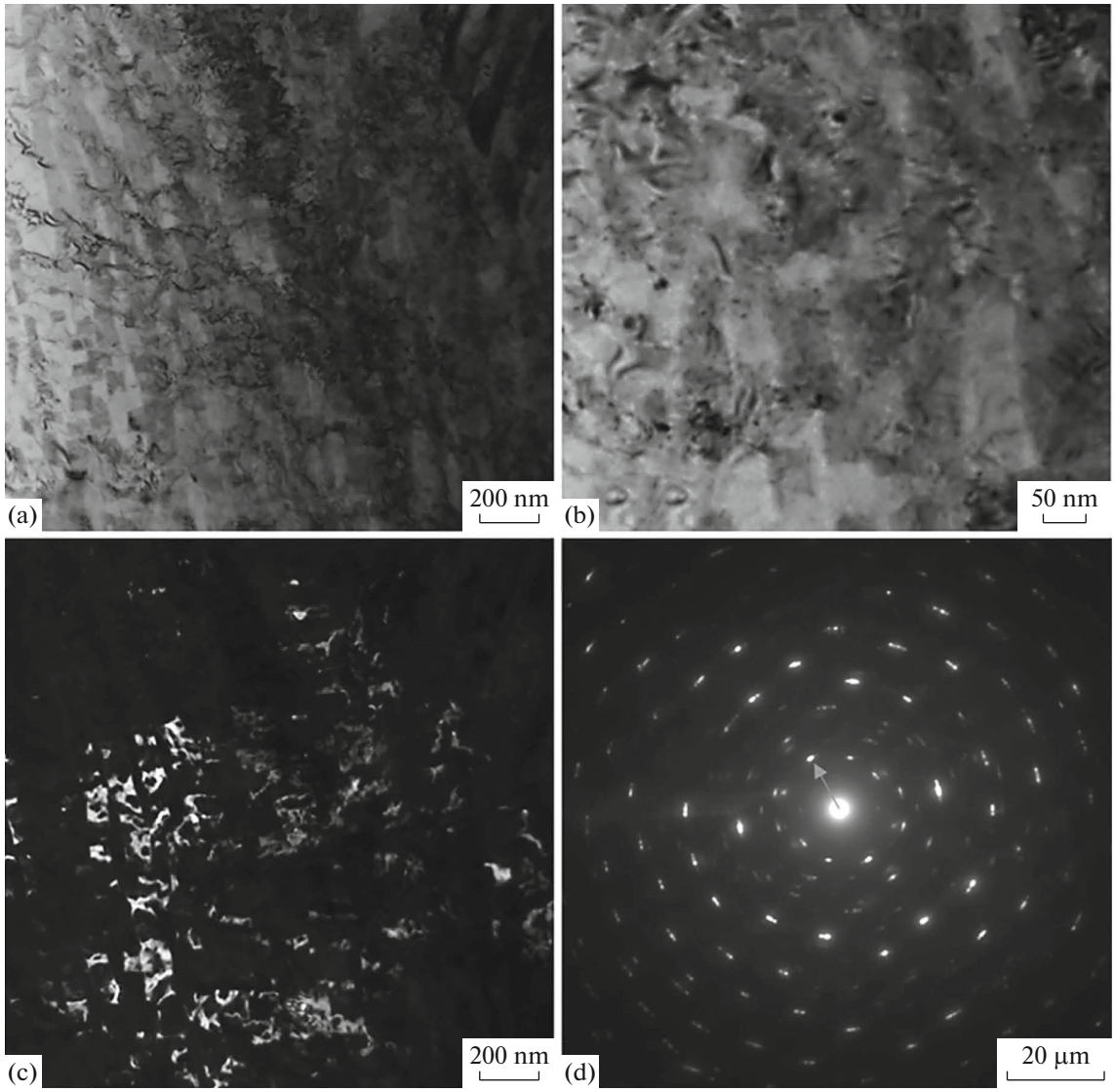


**Fig. 6.** Electron-microscopic images of the structure of the surface layer of rail steel: (a, b) bright-field images, (c) dark-field image taken with coincident [110] α-Fe and [031] $Fe_3C$ reflections, and (d) electron diffraction pattern (arrow indicates the reflection used to take the dark-field image).

cementite lamellae is their dissolution followed by the precipitation of iron carbide nanoparticles in ferrite lamellae (Fig. 7).

## CONCLUSIONS

(1) The structure of DT400IK rails made of E90KhAF steel in the initial state is represented by pearlite grains of predominantly lamellar morphology with insignificant primary cementite inclusions.

(2) After long-term operation, a dislocation substructure is observed in the ferrite lamellae of pearlite colonies, and the scalar dislocation density in the substructure increases as the fillet surface is approached, reaching a maximum at a distance of 2 mm from the surface.

(3) Stress concentrators are pearlite grain boundaries (intraphase boundaries) and ferrite and cementite lamella boundaries (interphase boundaries); the average transverse sizes of extinction contours change nonmonotonically as they move away from the surface and reach minimum values at a depth of 2 mm.

(4) The number of stress concentrators having formed at interphase boundaries is maximal at the fillet surface.

(5) The following two mechanisms of destruction of cementite lamellae were revealed: the dissolution of lamellae with the motion of carbon atoms to moving dislocations and the cutting of cementite lamellae by moving dislocations. Both mechanisms are operative in the surface layer of the fillet, and at a depth of

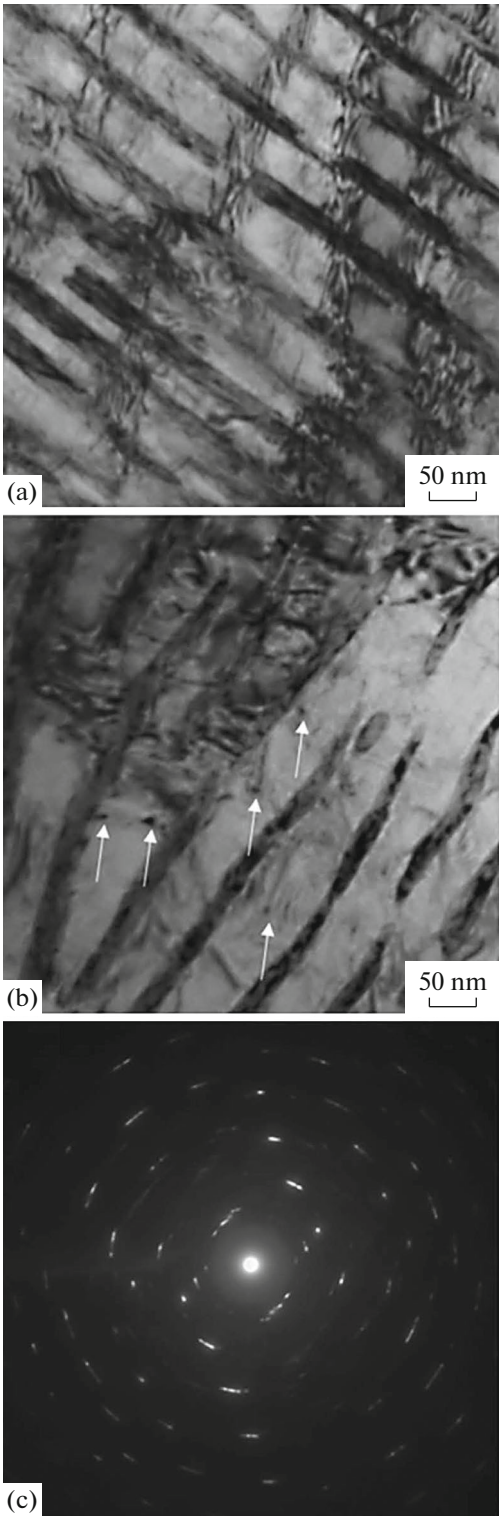


**Fig. 7.** Electron-microscopic images of the structure of rail steel at a distance of 2 mm from the fillet surface: (a, b) bright-field images; (c) electron diffraction pattern to (a). The arrows in (b) indicate rounded cementite particles located in the volume of ferrite lamellae.

2 mm, and the main mechanism for the destruction of cementite lamellae is the dissolution mechanism.

(6) The revealed quantitative laws of the formation of gradient structural-phase states and dislocation substructures in the surface layers of rails made of hypereutectoid steel after long-term operation can be useful for certifying DT400 IK rails and ensuring their guaranteed rail-carried tonnage of 2–2.5 bln t.

## FUNDING

This work was supported by ongoing institutional funding. No additional grants to carry out or direct this particular research were obtained.

## CONFLICT OF INTEREST

The authors of this work declare that they have no conflicts of interest.

## REFERENCES

1. A. A. Yuriev, Yu. F. Ivanov, V. E. Gromov, Yu. A. Rubannikova, M. D. Starostenkov, and P. Y. Tabakov, *Structure and Properties of Lengthy Rails after Extreme Long-Term Operation* (Materials Research Forum LLC, Millersville, 2021).
2. W. Lojkowski, Y. Millman, S. I. Chugunova, I. V. Goncharova, M. Djahanbakhsh, G. Bürkle, and H.-J. Fecht, "The mechanical properties of the nanocrystalline layer on the surface of railway tracks," Mater. Sci. Eng., A **303** (1, 2), 209–215 (2003).
3. Yu. Ivanisenko and H. J. Fecht, "Microstructure modification in the surface layers of railway rails and wheels: effect of high strain rate deformation," Steel Tech. **3** (1), 19–23 (2008).
4. J. Takahashi, K. Kawakami, and M. Ueda, "Atom probe tomography analysis of the white etching layer in a railtrack surface," Acta Mater. **58**, 3602–3612 (2010).
5. S. B. Newcomb and W. M. Stobbs, "A transmission electron microscopy study of the white-etching layer on a railhead," Mater. Sci. Eng. **66**, 195–204 (1984).
6. M. Ishida, "Rolling contact fatigue (RCF) defects of rails in Japanese railways and its mitigation strategies," Electron. J. Str. Eng. **13**, 67–74 (2013).
7. M. Steenbergen and R. Dollevoet, "On the mechanism of squat formation on train rails: Part I. Origination," Int. J. Fatigue **47**, 361–372 (2013).
8. S. Pal, C. Valente, W. Daniel, and M. Farjoo, "Metallurgical and physical understanding of rail squat initiation and propagation," Wear **284**, 30–42 (2012).
9. Y. F. Ivanov, V. E. Gromov, A. A. Yur'ev, A. M. Glezer, N. A. Popova, O. A. Peregudov, and S. V. Konovalov, "Contributions of various mechanisms to the hardening of differentially quenched rails during long-term operation," Russ. Metall. (Metally) **2018** (10), 985–989 (2018).
10. V. E. Gromov, Yu. F. Ivanov, R. V. Kuznetsov, A. M. Glezer, Yu. A. Shlyarova, and O. A. Peregudov, "Deformation transformation of the structure and phase composition of the rail surface during long-term

operation," Russ. Metall. (Metally) **2022** (10), 1157–1161 (2022).

11. K. V. Grigorovich, V. E. Gromov, R. V. Kuznetsov, Yu. F. Ivanov, and Yu. A. Shlyarova, "Formation of the fine structure of pearlitic steel during ultra-long plastic deformation," Dokl. Ross. Akad. Nauk Ser. Fiz. Tekh. Nauki **503**, 8–12 (2022).
12. N. A. Koneva and E. V. Kozlov, "Dislocation structure and physical mechanisms of hardening metallic materials," in *Advanced Materials. Structure and Investigations Methods*, Ed. by D. L. Meerson (TGU, Tula; MISiS, Moscow, 2006), pp. 267–320.
13. V. G. Gavriljuk, "Decomposition of cementite in pearlitic steel due to plastic deformation," Mater. Sci. Eng., A **345**, 81–89 (2003).
14. V. Ya. Tsellermaer, "Substructural and phase transformations during intense plastic deformation of metals," Steel Transl. **29** (12), 75–81 (1999).
15. Y. J. Li, P. Chai, C. Bochers, S. Westerkamp, S. Goto, D. Raabe, and R. Kirchheim, "Atomic-scale mechanisms of deformation-induced cementite decomposition in pearlite," Acta Mater. **59**, 3965–3977 (2011).
16. *Cementite in Carbon Steels*, Ed. by V. M. Schastlivtsev (UMTs UPI, Ekaterinburg, 2017).

*Translated by K. Shakhlevich*